A numerical study of the windstorm Klaus: sensitivity to sea surface temperature

Nazario Tartaglione[1,2,*], Rodrigo Caballero[1,3]

[1] *University College Dublin, School of Mathematical Sciences, Dublin, Ireland*

[2] *Current affiliation: University of Camerino, School of Science and Technology, Camerino, Italy*

[3] *Current affiliation: Stockholm University, Dept. of Meteorology and Bolin Center for Climate Research, Stockholm, Sweden*

Article history
Received November 21, 2013; accepted August 29, 2014.
Subject classification:
Atmosphere, Processes and Dynamics, Cyclone, Windstorm.

ABSTRACT

This article investigates the role of sea surface temperature (SST) as well as the effects of evaporation and moisture convergence on the evolution of cyclone Klaus, which occurred on January 23 and 24, 2009. To elucidate the role of sea surface temperature (SST) and air–sea fluxes in the dynamics of the cyclone, ten hydrostatic mesoscale simulations were performed by Bologna Limited Area Model (BOLAM). The first one was a control experiment with European Centre for Medium-Range Weather Forecasts (ECMWF) SST analysis. The nine following simulations are sensitivity experiments where the SST are obtained by adding a constant value by 1 to 9 K to the ECMWF field. Results show that a warmer sea increases the surface latent heat fluxes and the moisture convergence, favoring the development of convection in the storm. Convection is affected immediately by the increased SST. Later on, drop of mean sea level pressure (MSLP) occurs together with increasing of surface winds. The cyclone trajectory is not sensitive to change in SST differently from MSLP and convective precipitation.

1. Introduction

Windstorm Klaus occurred between January 23 and 24, 2009. When the storm landed on the coast of Western Europe it caused heavy damage in France and Spain [Liberato et al. 2011]. Analyzing the pressure maps and satellite images we can see that it was similar to cyclone Lothar that has been the subject of several papers [e.g. Wernli et al. 2002]. Klaus belongs to the group of cyclones called meteorological bombs as they deepen by at least 24 hPa in 24 h [Sanders and Gyakum 1980]. Extra-tropical cyclones tend to develop faster over the sea than over land [Sanders and Gyakum 1980, Ulbrich et al. 2009] and because of their rapid development it is challenging to forecast correctly their genesis and evolution [Sienkiewicz et al. 2004].

A possible influence of the upstream upper-level baroclinic processes on the explosive cyclogenesis of this kind of cyclones exists, as suggested by Uccellini [1986] for instance. Most of the meteorological bombs in the Atlantic Basin form just north of the Gulf Stream [Sanders and Gyakum 1980, Roebber 1984], showing the fundamental role of the sea surface temperature (SST). Lambert [1996] found a positive correlation between the number of northern hemisphere Pacific "intense" extra-tropical cyclones and SST gradients and a weak correlation in the Atlantic region. A sea surface with high temperature, beneath a cold atmosphere provides an abundant supply of heat and moisture that has a significant effect on the cyclone development [Danard 1983, 1986]. The latent heat release associated with condensation of water vapour definitely plays an important role through convection and/or the moist baroclinic processes [e.g. Davis and Emanuel 1991, Fantini 1991]. The impact of moist processes is not limited to cyclone thermodynamics but affects dynamics as well. Kuo and Low Nam [1990] for instance found that latent heat release can promote low level vorticity in meteorological bombs.

There is a huge literature on the impact of SST on tropical storms [e.g. Emanuel 2005], however the effects of SST on extra-tropical cyclones has been the object of only a few case studies [e.g. Danard 1986, Giordani and Caniaux 2001, Ren et al. 2004, Booth et al. 2012, Ludwig et al. 2014]. Indirect assessment of SST impact on extra-tropical cyclone intensity can be found in a few climatological studies, where a moderate positive impact of SST on the number of intense storms is found [Semmler et al. 2008a]. Climate change research also assesses indirectly the role of SST, but the results seem to be controversial. Semmler et al. [2008b] and

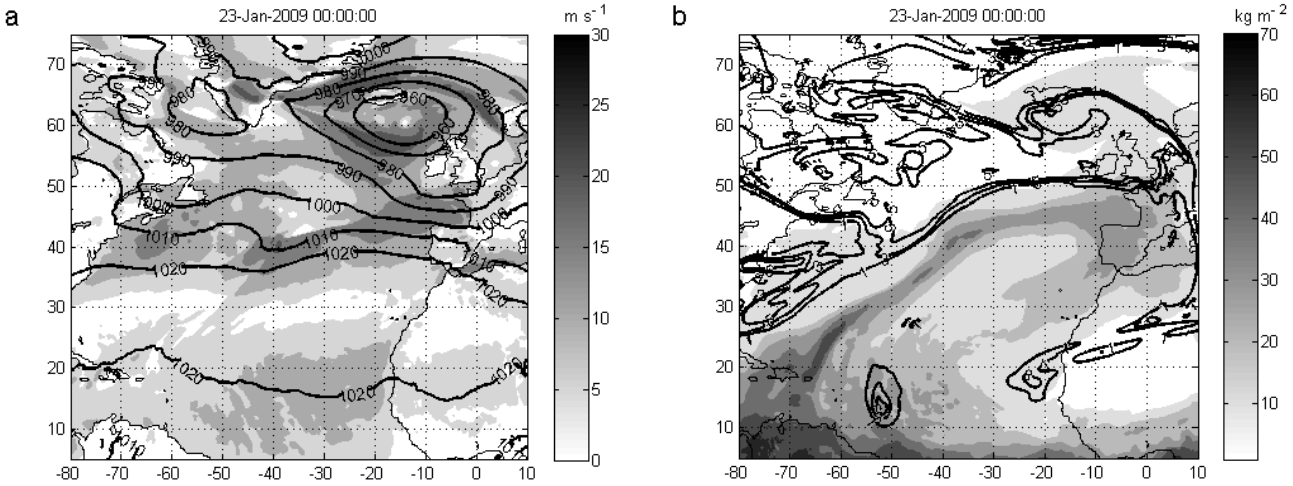

Figure 1. ECMWF analysis of MSLP (solid line) [hPa] and 10 m wind speed [$m\ s^{-1}$] (shaded) (a) and PV (solid line) at 300 hPa [PV unit], and TCWV (shaded) [$kg\ m^{-2}$] (b) at 00 UTC 23.

Leckebusch et al. [2006], for example, found a positive increase in the number of extra-tropical cyclones in a warmer climate, whereas the findings of Bengtsson et al. [2006] found a reduced number of storms, especially the weaker ones and no change in cyclone intensity. However the number of intense cyclones in Semmler et al. [2008b] in their control experiment is very small and the increment observed in a warmer climate was not so high as to be significant.

One of the motivations for this study was to understand how possible scenarios of warmer oceans might modify the evolution and the strength of extra-tropical storms. The Earth has already experienced a warmer climate in the past. For instance, in a recent data-model comparison for the early Eocene, Huber and Caballero [2011] found that the best-fit model simulation had a global-mean sea surface temperature of about 31°C, over 15°C warmer than today. In this study the impact of sea surface temperature on the evolution of cyclone Klaus is analyzed by means of numerical simulations. Changes in surface heat fluxes and moisture convergence will also be investigated in order to evaluate their contribution to the storm's evolution. Although results presented here cannot be extended to all cases, they may give us indications of the behavior of meteorological bombs when an increase of SST is taken into account.

The meteorological event together with a brief description of the model and the experimental design of the simulations is presented in Section 2. The numerical results are discussed in Section 3. The conclusions will be drawn in Section 4.

2. Synoptic description and experimental set up

The data used for the synoptic description are the 6 hourly 0.5° European Center for Medium Range Weather Forecast (ECMWF) analyses; they were also used for the initial and boundary conditions of the limited area model. The cyclone started as a perturbation of a frontal line that extended from the Caribbean to the British Isles. This perturbation can already be seen at 00 UTC 23 (around 40° west, 40° south, Figure 1a). Along the temperature front (not shown) high values of total column water vapour (TCWV) characterized this long frontal line (Figure 1b). The genesis of the cyclone occurred immediately south of the region with high 300 hPa potential vorticity (PV) values and no preliminary upper level perturbation was present over the cyclogenetic area (Figure 1b). However a strong cross front shear was associated with the location of initial cyclogenesis (not shown). Sinton and Mechoso [1984] suggested that such shears may provide most of the energy in the development of shallow frontal cyclogenesis. Figure 2 shows the synoptic situation at 00 UTC 24 when the cyclone was over the Bay of Biscay (Figure 2a), the 10 m wind speed reached its maximum intensity when the mean sea level pressure reached its minimum value. The cyclone moved along this frontal region of high TCWV. The cyclone collected water vapour (Figure 2b) during its path as indicated by the cyclonic curvature of the TCWV. At that time, the cyclone was embedded in a region of high PV values (Figure 2b). The interaction between forcing from upper levels, shown by high values of potential vorticity, and the underlying cyclone might be one cause of the cyclone deepening, as suggested for instance by Wernli et al. [2002] for cyclone Lothar or by Ludwig et al. [2014] for storm Xynthia. However, the hypothesis of Wernli et al. [2002] was not confirmed by Rivière et al. [2010] with their sensitivity experiment on storm Lothar. They showed that the absence of upper level perturbation did not inhibit cyclone Lothar from turning into a windstorm. The trajectory of Klaus occurred along the boundary of the high PV region (Figure 2b). However,

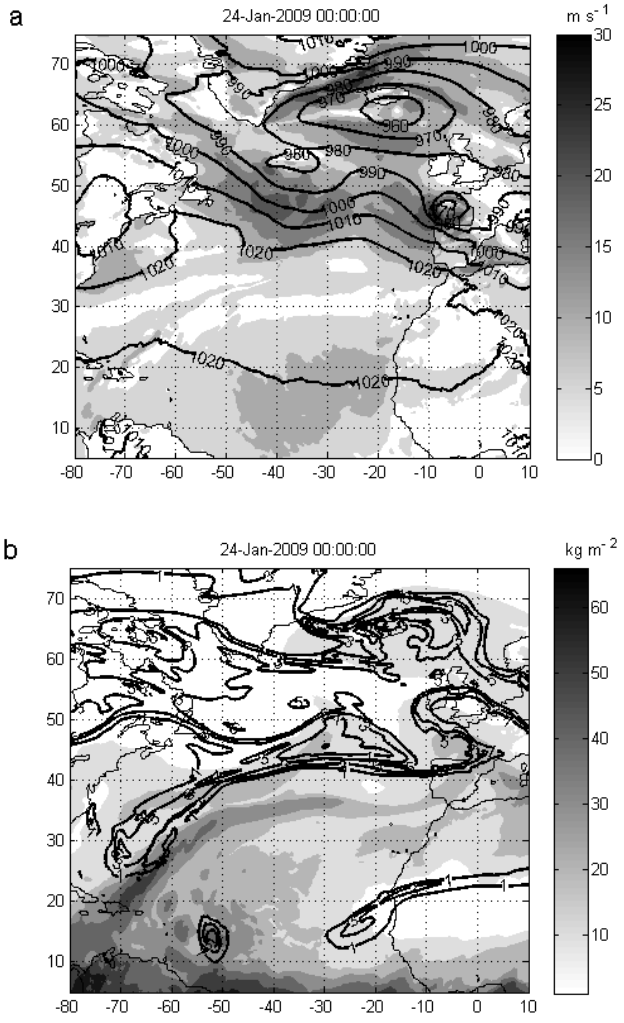

Figure 2. As Figure 1, but at 00 UTC 24.

as suggested by Dacre and Gray [2009] the development of some storms are mainly "low-level" forced, thus, the role of PV on meteorological bombs is not clear.

The trajectory of Klaus and the evolution of its MSLP minimum over time, as retrieved by ECMWF data, can be found in Liberato et al. [2011]. Moreover, Liberato et al. [2011] showed that the MSLP between 00 UTC 23 and 00 UTC 24 dropped by 34 hPa. Decreasing more than 24 hPa in 24 hours the cyclone can be classified as a meteorological bomb. The system made landfall in France during the early morning of the 24th. After landfall the pressure increased and the strong pressure gradients led to high winds in France and Spain. Liberato et al. [2011] gives a complete picture of the damage in those countries.

The simulations in this study was conducted by using the numerical weather model BOLAM (Bologna Limited Area Model) developed at the Institute for the Study of Atmosphere and Climate of the Italian National Research Council [e.g. Buzzi and Foschini 2000].

A control simulation (SST0) was performed followed by nine other runs in which the SST was increased from 1 K (SST1) to 9 K (SST9). Hereafter this increment will be also referred to as an "anomaly". Most of these variations may seem too large and unrealistic even in a warmer climate; however it is our intention to explore how large the effects of such SST variations might be on the development, in terms of MSLP and wind speeds, of a meteorological bomb like Klaus.

The numerical simulations started at 00 UTC 23. Six-hourly 0.5° ECMWF anayses were provided as initial and boundary conditions and the model was run in hind-cast mode. The model domain was 320×162 grid points with horizontal and vertical resolutions of 30 km and 40 σ-levels. Even though there was no interest in analyzing the sensitivity of the simulations to the grid resolution, the model was run at two different domains and resolutions, the former with a domain covering Western Europe with 15 km horizontal resolution and the latter covering most of the North-Atlantic basin and the Western Europe with 30 km horizontal resolution (Figure 3). A realistic prediction of this cyclone was only obtained once the initial perturbation was in the domain, i.e. by using the second and larger domain.

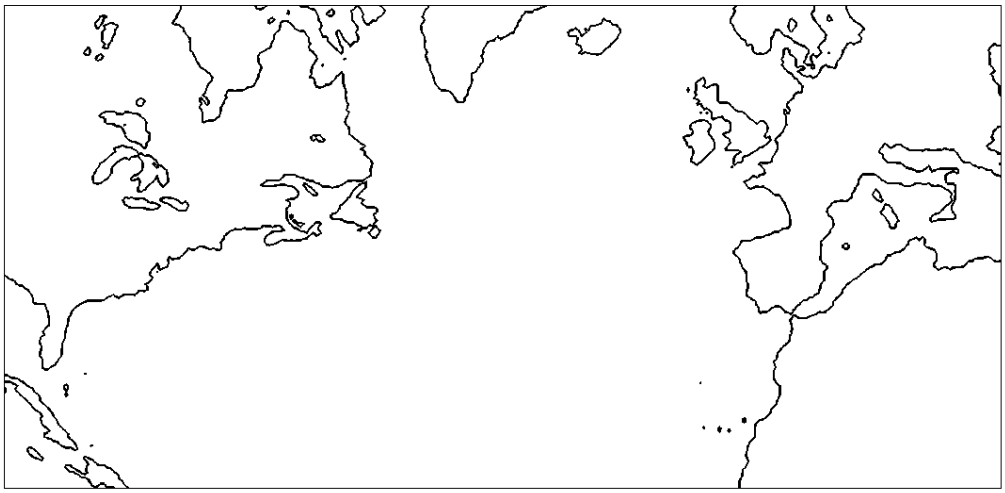

Figure 3. BOLAM domain.

The smaller domain with a higher resolution (15 km), but not containing the initial perturbation, gave a MSLP minimum of 984 hPa, larger than the 974 hPa obtained by the domain and horizontal resolution (30 km) used in this paper. Since our domain is quite extensive, analyses were performed on data of a limited region of 101×101 grid points that moved along with the cyclone.

3. Role of SST on storm evolution

In this section the simulated mean sea level pressure, precipitation and wind speeds are compared as functions of SST as well as the modeled surface latent heat and moisture convergence. This comparison covers the first 36 hours of the storm evolution, until the cyclone was over France.

3.1. Pressure, 10 m wind speed and precipitation: sensitivity to SST

Figure 4 shows the mean sea level pressure at 00 UTC 24, for the control (SST0) and SST9 experiments over the Bay of Biscay, after 24 hours of simulation. The simulated cyclone trajectories of the 10 experiments (from SST0 to SST9) did not show significant differences, with the cyclone center all ending, at 00 UTC 24, over the Bay of Biscay. This result is different, for example, from that found by Giordani and Caniaux [2001] where a significant change was observed in the trajectory of another cyclone when compared to the control simulation, in an experiment on warmer sea surfaces.

With warmer SST, a change in cyclone dynamics and physics is expected. This change can be analyzed using a few meteorological parameters. Figure 5 shows the evolution of the MSLP minimum (Figure 5a) and the ratio between convective and total precipitation (Figure 5b), computed in the 101×101 grid points box that moves with the cyclone. The minimum MSLP, at 00 UTC 24, simulated by BOLAM, in the control run, is 10 hPa higher than that retrieved by ECMWF analysis. This might be due to the coarse resolution. However, the aim of this paper is to study sensitivity to SST rather than to provide a perfect simulation of the storm.

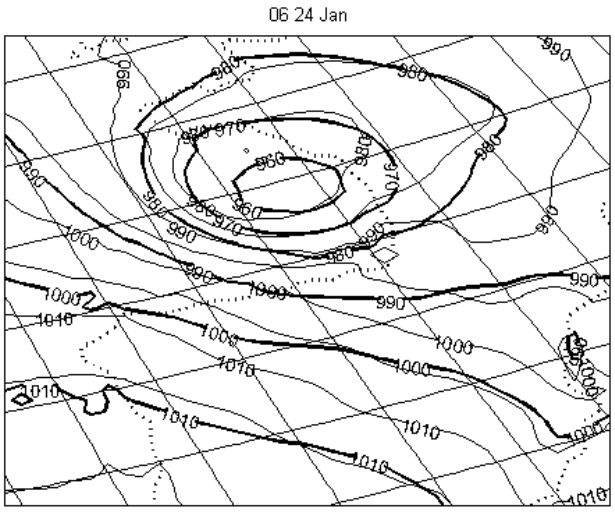

Figure 4. MSLP [hPa] for control experiment SST0 (thin line) and experiment SST9 (thick line) at 00 UTC 24, when the cyclone is over the Bay of Biscay.

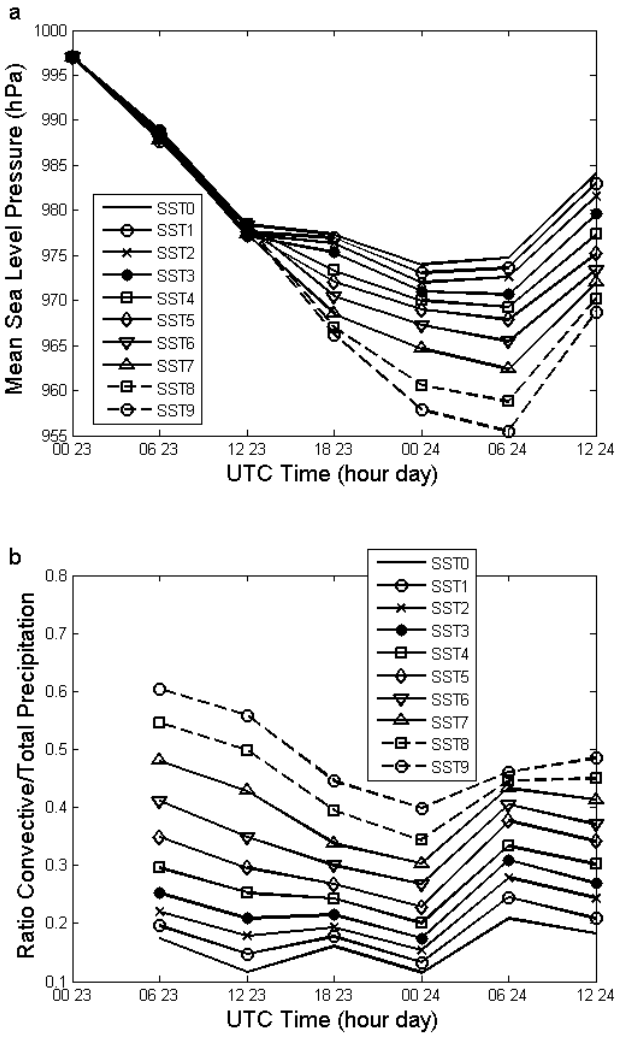

Figure 5. Maximum of 10 m wind speed [$m\ s^{-1}$] (a) and ratio convective / total precipitation (b) in a domain following Klaus during its evolution as a function of SST anomaly.

In the model, SST influenced the convective precipitation from the beginning (Figure 5b), whilst it impacted on the MSLP only at a later stage in the simulations (Figure 5a). The cyclogenesis was due to classic baroclinic instability, but it is very likely that later on air-sea-interaction processes played an important role in deepening this meteorological bomb, as water vapour triggered convective instability. This instability is enhanced with warmer SST. The relationship between convection and cyclone deepening was noted, for example, by Tracton [1973]. Gyakum and Barker's research [1988] on a meteorological bomb attributes the phases of rapid deepening to convection. The relationship between high convective precipitation and the decrease in MSLP of some extra-tropical cyclones might

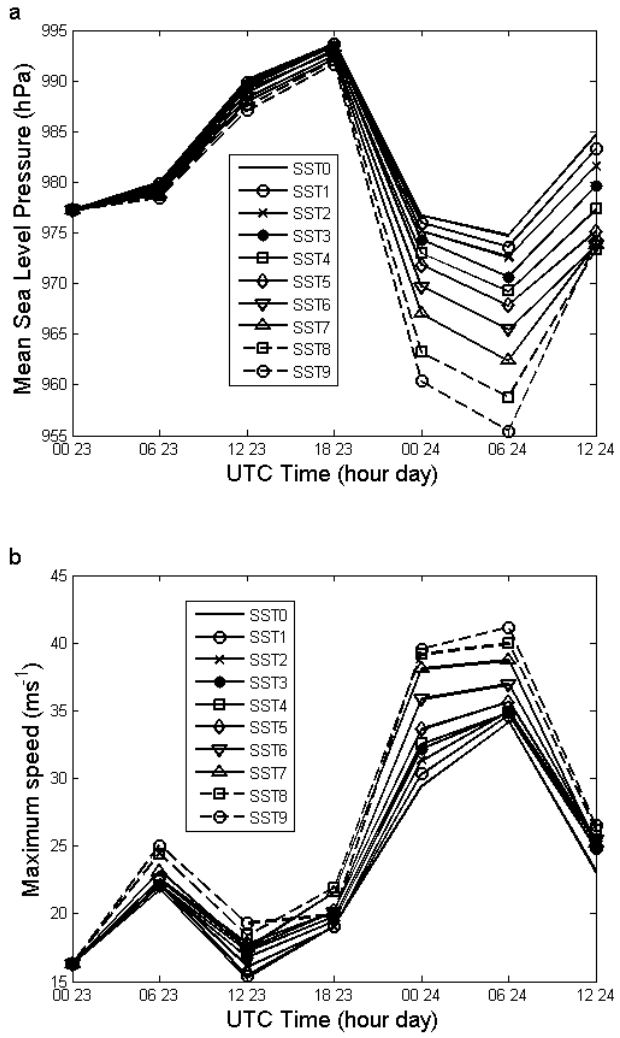

Figure 6. Minimum of MSLP [hPa] (a) and maximum of 10 m wind speed [$m\ s^{-1}$] (b) over the Bay of Biscay as a function of SST anomaly.

be related to the CISK [Danard 1983] or to a similar mechanism like the moist quasi-geostrophic baroclinic instability formulated by Mak [1982]. The intense latent-heat released during the condensation of water vapour in the convection may further induce cyclone deepening. The deeper pressure minimum and the corresponding increased pressure gradient favor a more intense low-level wind speed and, consequently, sea surface fluxes, inducing a positive feedback [Emanuel et al. 1994]. Thus, the warmer the sea surface, the more vigorous the feedback mechanism and the deeper the cyclone. Figure 5a shows that MSLP variation with SST is not linear. During the first 12 hours the impact of SST on the MSLP is not significant, but it becomes more important over time. When the temperature is larger than 5 K the MSLP drop increases significantly with the SST, suggesting a non-linear effect due to water vapour associated with latent heat released by condensation of water vapour during convection. In fact, the convective precipitation, for anomalies of 5 K and above, is a significant part of the total precipitation (Figure 5b). The sea surface is the main source of the water vapour, whose condensation within the cyclone provides the energy necessary to increase the intensity of the cyclone.

When the cyclone was over the Bay of Biscay, the MSLP reached the minimum value, whereas over the land the cyclone weakened. Figure 6 shows MSLP and wind speed over the Bay of Biscay. The cyclone reached its maximum intensity over the Bay of Biscay, between 00 UTC and 06 UTC 24 (Figure 6). In this case a fixed box (21×21 grid points) covering the Bay of Biscay was used to obtain the values shown in Figure 6. Close to French coastline the roughness difference between sea and land increases the pressure gradient causing strong winds. However wind speeds are higher with a warmer sea because it favors cyclone deepening (Figure 6b).

3.2. Surface latent heat fluxes

Air-sea interaction has long been recognized as one of the factors leading to explosive cyclones. The oceans provide heat, through sensible and latent surface heat fluxes, and water vapour through the evapo-

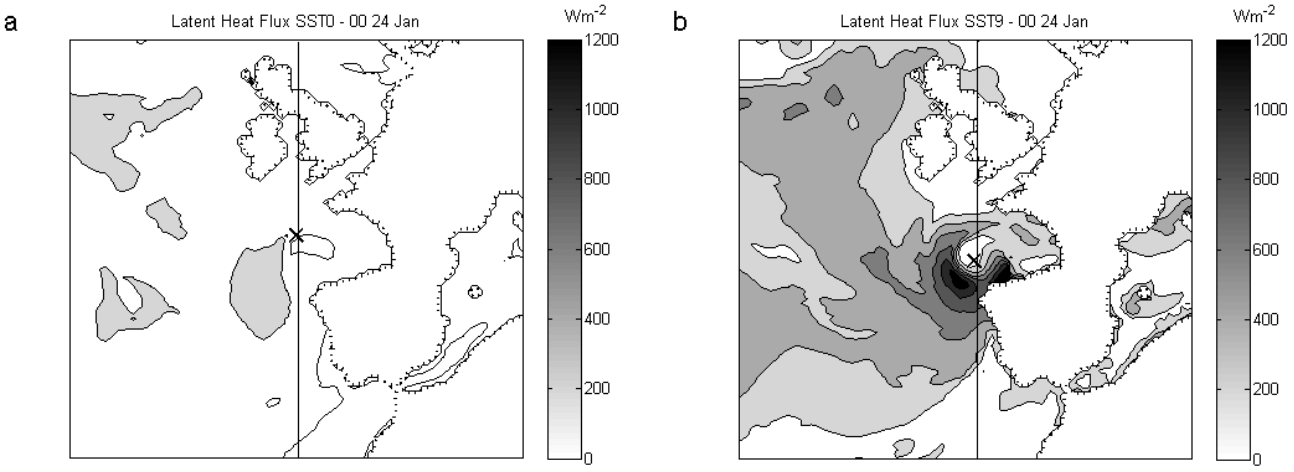

Figure 7. Surface latent heat flux [W m^{-2}] at 12 UTC 23 for simulations SST0 (a) and SST9 (b). The sign **X** indicates the cyclone center, the vertical line is for the cross section.

ration and convergence of moisture. Evaporation is associated with positive surface latent heat flux, i.e. the ocean provides energy to the atmosphere.

Figure 7 shows the surface latent heat flux for simulations SST0 and SST9 at 00 UTC 24. The surface latent heat fluxes in the control simulation are weak (Figure 7a) compared to the SST9 experiment (Figure 7b). With larger SST anomalies there are high values of surface latent heat fluxes very close to the cyclone (Figure 7b), in fact two surface latent heat flux maxima are obvious, one at the south-east, and the other just in the wake of the cyclone in accordance with the results found by Petterssen et al. [1962]. The larger the SST anomalies, the higher the surface latent heat fluxes; an unsurprising result, not only because of a warmer sea, but also because of the deeper cyclone and higher wind speed. The highest values of surface latent heat fluxes close to the cyclone center reach about 1200 $W\ m^{-2}$ in the SST9 experiment (Figure 7b), exceeding those of the control simulation (Figure 7a). These values correspond to about 1.7 $mm\ h^{-1}$ in terms of evaporation rate. The surface latent heat fluxes are strong in the region of the cold air outbreak behind the atmospheric front. As we will see afterward 1.7 $mm\ h^{-1}$ is much less than the contribution of the moisture convergence to the water vapour.

Figures 8 for SST0 and 9 for SST9 show meridional vertical cross sections along the vertical line in Figure 7 at 00 UTC 24, showing: potential temperature and vertical velocity (omega) (panel a); wind zonal component (panel b); wind meridional component (panel c); and specific humidity (panel d). After 24 hours of simulation we observe how the adiabatic flow follows the potential temperature contours that come from the south towards the cyclone center. In the SST0 simulation, a region of strong vertical velocity is visible in the center of the cyclone (Figure 8a). SST9 shows a warmer atmosphere because of the energy that oceans exchange with the atmosphere. Moreover, there are more updrafts in SST9, not only at the center of the cyclone, but also in areas to the north and south of the cyclone (Figure 9a). For the SST0 and SST9 the potential temperature shows a cooling region just south of the main updraft, but in the SST9 this cooling is more marked, probably due to more rainfall evaporation. SST0 wind components (Figures 8b and 8c) are stronger and gradients larger than SST9 winds (Figures 9b and 9c). Convergent winds together with moisture advection are favorable conditions for convection. The specific humidity values in SST9 (Figure 9d) are larger and extend higher altitudes than SST0 (Figure 8d).

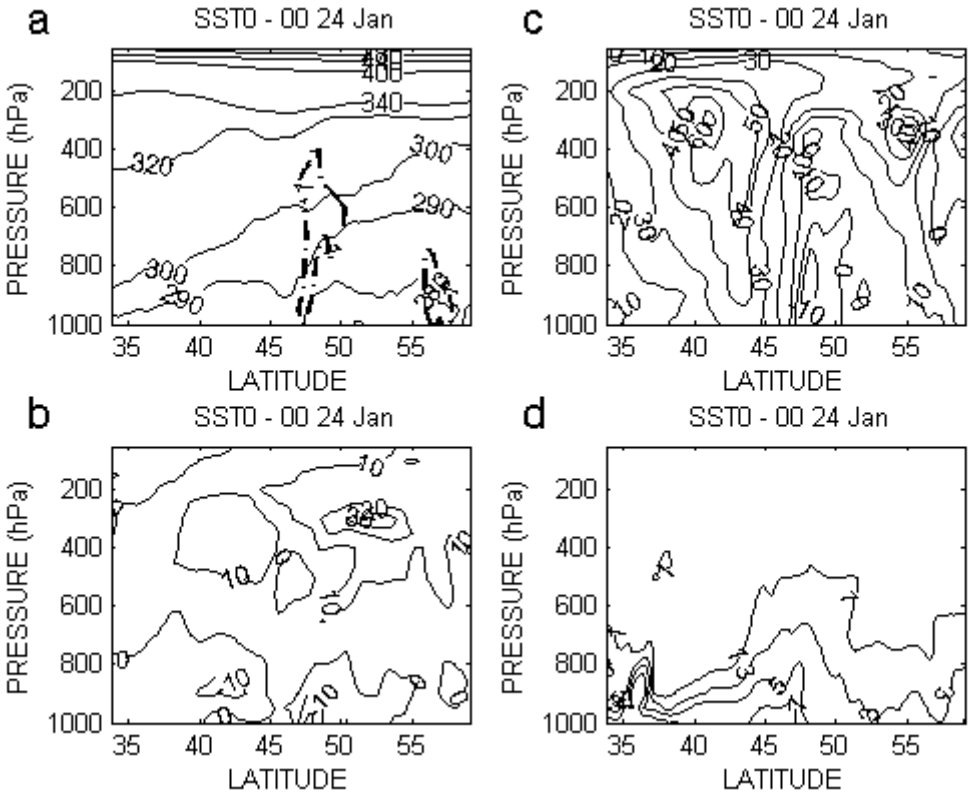

Figure 8. Vertical cross section along the meridional direction (see Figure 7) of potential temperature (solid line) [*K*] and vertical velocity (omega) (dashdot line) [$Pa\ s^{-1}$] (a), wind zonal component (b) and wind meridional component (c) [$m\ s^{-1}$] and specific humidity [$g\ kg^{-1}$] (d) at 00 UTC 24 for the experiment SST0.

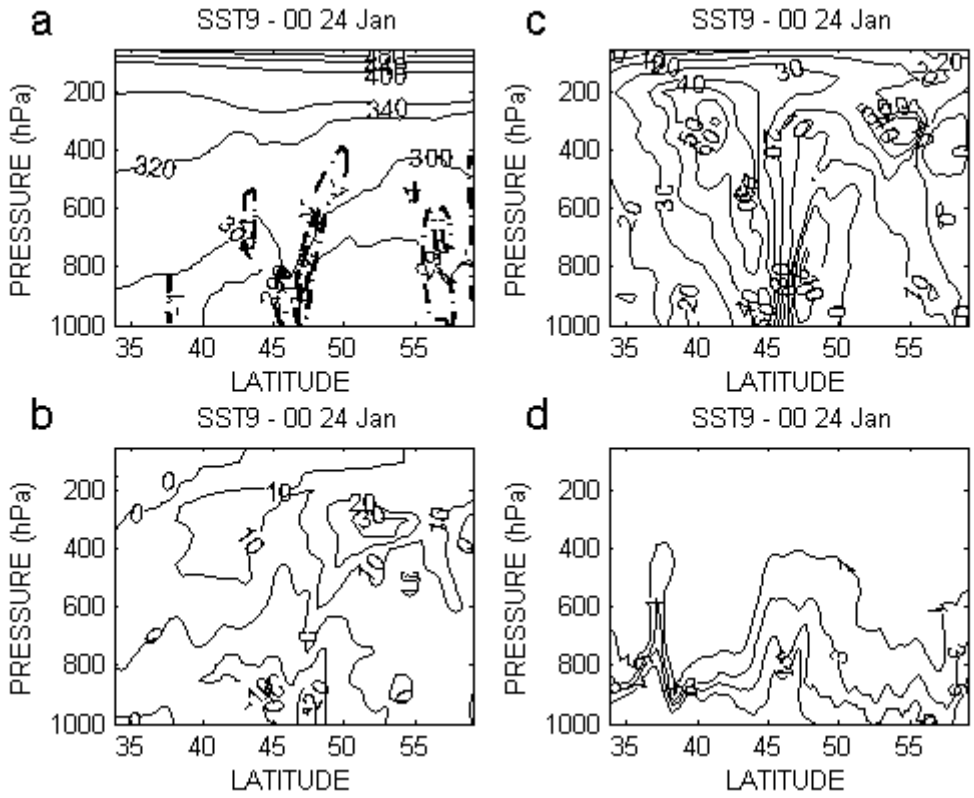

Figure 9. As Figure 8 but for the experiment SST9.

3.3. Moisture convergence

There are two mechanisms that provide humidity in the atmospheric boundary layer: evaporation and moisture convergence. Evaporation from the sea is related to the surface latent heat flux, as shown in the previous section.

Moisture convergence may be written as

$$M_c = \int_0^{Pbl} \nabla \cdot V_f \, q \frac{dp}{g} + k \cdot \nabla \times \frac{q}{f} \tau = H + W \quad (1)$$

where the vector V_f defined as the friction free wind in the atmospheric boundary layer, V_f is computed by means of the following formula:

$$V_f = V_g + \frac{k}{f} \times \frac{dV}{dt}$$

where **k** is the vector along the z direction. The symbol ∇ represents the divergence operator, q represents the specific humidity, f represents the Coriolis parameter and g represents gravity acceleration. The first term H on the right-hand side of (1) represents vertically-integrated low-level moisture convergence. Integration in the boundary layer is calculated using the pressure p variable. The term W relates to the rotational term of moisture convergence, where the vector **τ** represents surface stress. The moisture convergence measure unit is $kg\ m^{-2}\ s^{-1}$. It is easy to show that $kg\ m^{-2}$ is equivalent to

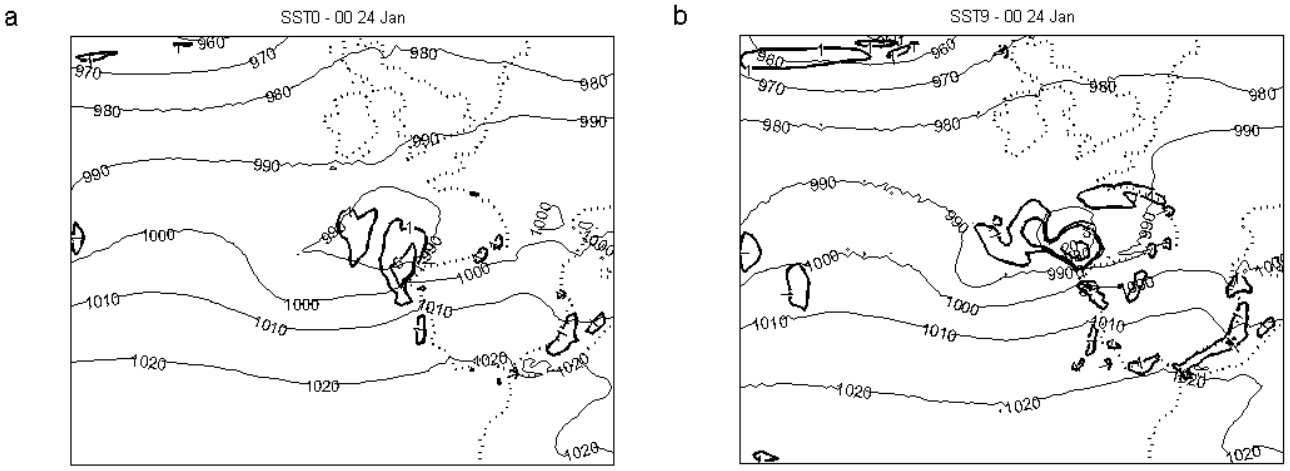

Figure 10. The contribution of $W\ [mm\ h^{-1}]$ to the moisture convergence (Equation 1) at 00 UTC 24 for experiments SST0 (a) and SST9 (b).

mm of water: multiplying and dividing by 3600, $kg\ m^{-2}\ s^{-1}$ transforms into $mm\ h^{-1}$. The use of $mm\ h^{-1}$ gives an immediate insight into the effects of moisture convergence on precipitation, although not all the moisture transforms into precipitation.

The analysis of both terms *W* and *H* shows that the term *W* is much larger than H. At 00 UTC 24 W is about 5 $mm\ h^{-1}$ for the SST0 experiment, whereas it reaches 20 $mm\ h^{-1}$ for SST9 (Figure 10). These values are much larger than those obtained by evaporation (1.7 $mm\ h^{-1}$). The term *H* is an order of magnitude less than *W* and it has values of 1 $mm\ h^{-1}$ at few grid points and only for SST8 and SST9. Once more vapour reaches the atmosphere it contributes to the diabatic processes that in cyclones like Klaus play an important role. Fink et al. [2012] found that, for the windstorm Klaus, the contribution of diabatic heating to cyclone deepening was larger than that of baroclinic instability.

4. Conclusions

In this paper, the sensitivity of cyclone Klaus to the SST was studied by mean of limited area model initialized by ECMWF analysis. Ten simulations were performed, the first one with ECMWF SST field (SST0 simulation) and nine other simulations using SST analysis raised by 1 to 9 K. The modeled atmospheric parameters: precipitation, MSLP and contributions to water vapour were compared. They showed very different behavior with respect to the SST. Increasing SST leads to more evaporation, enhancing convection in the cyclone. The surface latent heat fluxes, higher in SST9 than SST0, modify the boundary layer triggering an efficient mechanism for convective destabilization. The latent heat released by condensation of water vapour, during convective processes, has an effect on the drop in MSLP. Moreover, whereas convection is immediately influenced by SST and precipitation becomes more convective in SST with higher temperatures, the drop in MSLP is only affected by higher SST at a later stage. It takes some time for SST to have a significant effect on the MSLP (Figure 5a). The importance of SST on extra-tropical storms has recently been demonstrated by storm Xynthia [Ludwig et al. 2014]. Increasing SST leads to more moisture in the atmosphere contributing to increase the latent heat released by water vapour condensation. The importance of diabatic processes on storm development is recognized by several studies [e.g. Fink et al. 2012, Ludwig et al. 2014]. High surface latent heat fluxes, which increase with SST, are necessary for the initial storm intensification, but the contribution of evaporation is less than that of moisture convergence; hence once the storm starts to produce strong winds, these increase water vapour also through moisture convergence. Thus, both evaporation and moisture convergence play an important role in cyclone intensification through diabatic processes, especially in experiments with high SST anomalies.

Acknowledgements. This work has been funded by Science Foundation Ireland under the contract SFI-GEOF252 "Present and future statistics of extreme European storms in a large ensemble of high-resolution atmosphere model simulations". Irish Centre for High-End Computing (ICHEC) is acknowledged for the computing time used to run the model. The authors acknowledge three anonymous reviewers for their useful comments and suggestions; a special thank goes to two of reviewers for their significant corrections they made to the manuscript. Andrea Buzzi and Piero Malguzzi are acknowledged for BOLAM.

References

Bengtsson, L., K.I. Hodges and E. Roeckner (2006). Storm tracks and climate change, J. Clim., 19, 3518-3543.

Booth, J.F., L. Thompson, J. Patoux and A.K. Kathryn (2012). Sensitivity of midlatitude storm intensification to perturbations in the sea surface temperature near the Gulf Stream, Mon. Wea. Rev., 140, 1241-1256.

Buzzi, A., and L. Foschini (2000). Mesoscale meteorological features associated with heavy precipitation in the southern Alpine region, Meteorol. Atmos. Phys., 72, 131-146.

Danard, M.B. (1983). On the role of the boundary planetary layer in cyclogenesis over the ocean, Atmosphere-Ocean, 21, 466-470.

Danard, M.B. (1986). On the sensitivity of predictions of marittime cyclogenesis to convective precipitation and sea temperature, Atmosphere-Ocean., 24, 52-72.

Dacre, H.F., and S.L. Gray (2009). The spatial distribution and evolution characteristics of North Atlantic cyclones, Mon. Weather Rev., 137 (1), 99-115; ISSN 0027-0644, doi:10.1175/2008MWR2491.1.

Davis, C.A., and K.A. Emanuel (1991). Potential vorticity diagnostics of cyclogenesis, Mon. Wea. Rev., 119, 1929-1953.

Emanuel, K.A., J.D. Neelin and C.S. Bretherton (1994). On large-scale circulations in convective atmosphere, Q. J. Roy. Meteor. Soc., 120, 1111-1143.

Emanuel, K. (2005). Increasing destructiveness of tropical cyclones over the past 30 years, Nature, 436, 686-688.

Fantini, M. (1991). Baroclinic instability and induced air-sea heat exchange. Tellus, 43A, 285-294.

Fink, A.H, S. Pohle, P. Knippertz and J. Pinto (2012). Diagnosing the influence of diabatic processes on the explosive deepening of extratropical cyclones over the North Atlantic, Geophys. Res. Lett., 39, L07803;

doi:10.1029/2012GL051025.

Giordani, H., and G. Caniaux (2001). Sensitivity of cyclogenesis to sea surface temperature in the northwestern Atlantic, Mon. Wea. Rev., 129, 1273-1295.

Gyakum, J.R. and E.S. Barker (1988). A case study of explosive subsynoptic-scale cyclogenesis, Mon. Wea. Rev., 116, 2225-2253.

Huber, M., and R. Caballero (2011). The early Eocene equable climate problem revisited, Climate Past, 7, 603-633.

Kuo, Y.H., and S. Low-Nam (1990). Prediction of nine explosive cyclones over the western Atlantic Ocean with a regional model, Mon. Wea. Rev., 118, 3-25.

Lambert, S.J. (1996). Intense extratropical northern hemisphere winter cyclone events: 1899-1991, J. Geophys. Res., 101 (D16), 21319-21325.

Leckebusch, G.C., B. Koffi, U. Ulbrich, J.G. Pinto, T. Spangehl and S. Zacharias (2006). Analysis of frequency and intensity of European winter storm events from a multi-model perspective, at synoptic and regional scales, Clim. Res., 31, 59-74.

Liberato, M.L.R., J.G, Pinto, I.F. Trigo and R.M. Trigo (2011). Klaus - an exceptional winter storm over northern Iberia and southern France, Weather, 66, 330-334.

Ludwig, P., J.G. Pinto, M. Reyers and S.L. Gray (2014). The role of anomalous SST and surface fluxes over the southeastern North Atlantic in the explosive development of windstorm Xynthia, Q. J. Roy. Meteor. Soc., 140, 1729-1741.

Mak, M. (1982). On moist quasi-geostrophic baroclinic instability, J. Atmos. Sci., 39, 2028-2037.

Petterssen, S., D.L. Bradbury and K. Pedersen (1962). The Norwegian cyclone models in relation to heat and cold sources, Geophys. Publ., 24, 243-280.

Ren, X., W. Perrie, Z. Long and J. Gyakum (2004). Atmosphere–Ocean coupled dynamics of cyclones in the midlatitudes, Mon. Wea. Rev., 132, 2432-2451.

Rivière, G., P. Arbogast, K. Maynard and A. Joly (2010). The essential ingredients leading to the explosive growth stage of the European wind storm Lothar of Christmas 1999, Q. J. Roy. Meteor. Soc., 136, 638-652.

Roebber, P.J. (1984). Statistical analysis and updated climatology of explosive cyclones, Mon. Wea. Rev., 112, 1577-1589.

Sanders, F., and J.R. Gyakum (1980). Synoptic-dynamic climatology of the "bomb", Mon. Wea. Rev., 108, 1589-1606.

Semmler, T., S. Varghese, R. McGrath, P. Nolan, S. Wang, P. Lynch and C. O'Dowd (2008a). Regional model simulation of North-Atlantic cyclones: present climate and response to increased sea surface temperature, J. Geophys. Res., 113, 02107; doi:10.1029/2006JD008213.

Semmler, T., S. Varghese, R. McGrath, P. Nolan, S. Wang, P. Lynch and C. O'Dowd (2008b). Regional climate model simulations of North Atlantic cyclones: frequency and intensity changes, Clim. Res., 36, 1-16.

Sienkiewicz, J.M., D.S. Prosise and A. Crutch (2004). Forecasting oceanic cyclones at the NOAA Ocean Prediction Center. Preprints, Symp. on the 50th Anniversary of Operational Numerical Weather Prediction, College Park, MD, Amer. Meteor. Soc., CD-ROM, 5.7.

Sinton, D.M., and C.R. Mechoso (1984). Non linear evolution of frontal wave, J. Atmos. Sci., 41, 3501-3517.

Tracton, M.S. (1973). The role of cumulus convection in the development of extratropical cyclones, Mon. Weather Rev., 101, 573-592.

Uccellini, L.W. (1986). The Possible influence of upstream upper-level baroclinic processes on the development of the *QE II* Storm, Mon. Wea. Rev., 114, 1019-1027.

Ulbrich, U., G.C. Lackebusch and J.G. Pinto (2009). Extra-tropical cyclones in the present and future climate: a review, Theor. Appl. Clim., 96, 117-131.

Wernli, H., S. Dirren, M.A. Liniger and M. Zillig (2002). Dynamical aspects of the life-cycle of the winter storm 'Lothar' (December 24-26, 1999), Q. J. Roy. Meteor. Soc., 128, 405-429.

*Corresponding author: Nazario Tartaglione,
University of Camerino, School of Science and Technology,
Camerino, Italy; email: nazario.tartaglione@unicam.it.